Damage of multilayer optics with varying capping layers induced by focused extreme ultraviolet beam

Alain Jody Corso, Paola Zuppella, Frank Barkusky, Klaus Mann, Matthias Müller et al.

Additional information on J. Appl. Phys.

Damage of multilayer optics with varying capping layers induced by focused extreme ultraviolet beam

Alain Jody Corso,[1,2] Paola Zuppella,[1] Frank Barkusky,[3,4] Klaus Mann,[3] Matthias Müller,[3] Piergiorgio Nicolosi,[1,2] Marco Nardello,[1,2] and Maria Guglielmina Pelizzo[1,2]

[1]*National Research Council of Italy, Institute for Photonics and Nanotechnology, via Trasea 7, 35131 Padova, Italy*
[2]*Department of Information Engineering, University of Padova, via Gradenigo 6/B, 35131 Padova, Italy*
[3]*Laser-Laboratorium Göttingen e.V, Göttingen, Germany*
[4]*KLA-Tencor, 5 Technology Dr., Milpitas, California 95035, USA*

Extreme ultraviolet Mo/Si multilayers protected by capping layers of different materials were exposed to 13.5 nm plasma source radiation generated with a table-top laser to study the irradiation damage mechanism. Morphology of single-shot damaged areas has been analyzed by means of atomic force microscopy. Threshold fluences were evaluated for each type of sample in order to determine the capability of the capping layer to protect the structure underneath. © *2013 Author(s). All article content, except where otherwise noted, is licensed under a Creative Commons Attribution 3.0 Unported License.* [http://dx.doi.org/10.1063/1.4807644]

I. INTRODUCTION

The interest in the very strong interaction between Extreme UltraViolet (EUV) radiation and matter, together the EUV photo-lithography industry, drives the research for development of optical elements able to manipulate short wavelength radiation useful especially in matter physics, solar physics, and photolithography. In the EUV region the use of nano-structured optical coatings is required;[1–4] in fact, since in this range conventional single layer coatings provide negligible reflectance near normal incidence, significant reflectance can be obtained only with multilayer (ML) structures. Such specific optical elements consist of periodic or aperiodic stacks, based on two or more materials in the nanometric scale, deposited on an ultra-smooth substrate. High performances, specific properties, long term stability, and resistance to high flux irradiation are pivotal technological issues.

At wavelengths longer than the Si–L absorption edge (12.4 nm) up to 35 nm, Mo/Si multilayers are widely used for their relatively high reflectance and stability, even though recently new couples of materials have been considered in this range.[5–7] The use of other materials is mandatory at shorter wavelengths.

Applications for multi-layer mirrors are in ultra-short pulse manipulation and in beam transport system for synchrotron and Free Electron Laser beamlines. Ultra-short light pulses can be generated by the interaction of femtosecond laser pulses at high power density with a gas jet; the ionization of the atoms in the laser field produces a spectrum of laser harmonics extending up to the x-ray spectral region. It has been demonstrated that High Order Harmonics (HOH) are emitted in a time corresponding to a short fraction of the fundamental laser period; thus, by selecting a portion of the HOH spectrum, a pulse with sub-femtosecond time duration can be obtained.[8,9] In general, harmonics have a phase mismatch characterized by a positive second order chirp.

Manipulation of such pulses is achieved by the use of multilayer mirrors able to obtain a temporal compression up to attosecond pulses by the harmonic phase mismatch compensation;[3,10–12] multilayer mirror optical schemes are also used in HOH generation setups to change the polarization state of the pulse.[13]

High brilliance EUV femtosecond pulses with unprecedented photon fluxes are emitted by Free Electron Lasers (FEL). Multilayers are key optical elements for such beam transport and manipulation.[14] The FEL FERMI in Trieste, Italy will use multilayer optics instead of a monochromator for wavelength selection, with improved performance in wavefront preservation and efficiency.[4,15] FERMI@ELETTRA is based on a high gain harmonic generation (HGHG) seeding scheme, an approach that provides highly intense radiation pulses whose temporal structure, spectral distribution, and photon energy are stable from pulse to pulse over the time. These properties of the FEL beam must be preserved up to the end-user stations by the use of ad-hoc optical systems: wavefront and pulse duration preservation, as well as improvement of monochromaticity and selection of spectral content, can be achieved in such FEL transport systems by the use of multilayers. Multilayer optics will be useful also to realize delay line systems able to split the beam and temporally shift one component with respect to the other.[16]

The stability of nanostructured coatings for all different applications during experimental operation has been investigated by different authors.[17–20] This task is of particular importance when related to FEL applications, due to the high average and peak power densities of these sources. Therefore, damage of Mo/Si multilayers by FEL irradiation has already been investigated, employing the DESY-FLASH facility.[21,22] In addition, first damage tests with a table top laser produced plasma source with the same wavelength (13.5 nm) and fluencies of the FEL beam,[19,20] but in the nanosecond pulse length regime has been carried out.

The performance of a multilayer in terms of hardness and throughput can be enhanced by adding proper capping layers and by novel designs based on aperiodic stacks.[23] Capped Mo/Si multilayers have been developed for the FERMI@ELETTRA beam transport system. Multilayer mirrors able to filter the third harmonic, while rejecting the fundamental, are foreseen in optical systems for pump and probe experiments.[24] Multilayers with high reflectance at third harmonics shall be used in the delay lines to control the temporal delay of the pulses.[4,15,16]

In the present experiment the attention was focused on the resistance of capped multilayers, evaluating the influence of the top layers on the damaging process, measuring the respective damage thresholds, and providing a comparison between capped and standard Mo/Si periodic stacks. The coatings were exposed to an EUV beam from a laser-produced plasma with nanosecond pulse duration, which was tightly focused using a Schwarzschild objective.

II. SAMPLES AND DAMAGE TESTING PROCEDURE

The fabricated structures are based on periodic Mo/Si MLs optimized for high efficiency at 13.5 nm wavelength, with a working angle of 45°. They are composed by 50 bi-layers with a period of $d = 10.2$ nm and a gamma ratio $\Gamma = 0.62$. On-top of the periodic stack, different aperiodic capping–layers (CL) were designed in order to improve the harmonics selection capabilities of the basic periodic structure using the optimization technique described previously.[16] The capping layer structures were optimized to increase the Fundamental Rejection Ratio (FRR), i.e., the ratio between the reflectance at the third harmonic (i.e., 13.5 nm) and the fundamental (i.e., 40.5 nm). In Table I, the capping-layer structures adopted in the experiment together with their experimental peak reflectance and FRR values measured at BEAR beamline in ELETTRA Synchrotron, Trieste, Italy are compiled.

The multilayer structures (one sample for each capping-layer) were deposited on 16 mm × 16 mm polished Si(100) substrates using a DC-magnetron sputtering facility described elsewhere.[25]

The samples have been exposed at Laser-Laboratorium Göttingen e.V. (Germany), with an experimental setup already described before[19] and sketched in Fig. 1.

The EUV radiation is generated by focusing a Nd:YAG laser (Innolas, 1064 nm wavelength, 8.8 ns duration, 700 mJ pulse energy) onto a solid gold target of 200 μm thickness deposited on a rotating Cu rod. The resulting plasma has a diameter of $\sim$50 μm with a high emission peak in the EUV range. A Schwarzschild objective, coated with Mo/Si
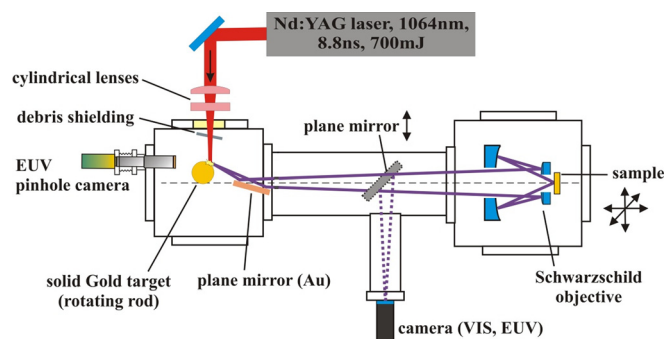

FIG. 1. Sketch of the laser produced plasma facility at Laser-Laboratorium Göttingen e.V. (Germany).

multilayers, filters the incident radiation to a narrow peak around 13.5 nm and focuses the radiation on the sample (demagnification 10×, maximum numerical aperture 0.4), providing fluencies up to several J/cm^2. The incidence angles on the sample range from 12.7° to 26.6°, with a mean angle of 20°. A plane mirror (Au coated silicon wafer, R $\sim$ 0.675 for grazing angle of 10°) is positioned between the source and the objective in order to protect the Mo/Si multilayers against possible contamination from laser plasma debris. The samples were mounted on a two axis translation stage in order to move the surface with respect to the impinging beam spot. The main experimental parameters are reported in Table II.

During the experiment the fluence was varied from 330 to 2220 mJ/cm^2 by changing the Nd:YAG voltage. For each fluence value, five single shot spots have been obtained as shown in the sketch reported in Fig. 2; an alphanumeric code is used to univocally identify each spot. Nature and the morphology of the damage have been investigated by a non-contact mode Atomic Force Microscope (AFM, model Park System XE70), obtaining a topographic map of the spots.

III. RESULTS AND DISCUSSION

A. Damage morphology

The appearance of the damage areas on CL1, CL2, and CL3 samples is very similar, and for this reason the AFM topographies taken for the Pd/a-Si capped sample and reported in Fig. 3 can be considered as representative for all Pt- and Pd-based MLs; in Fig. 4 a sequence of selected height profiles is also reported. The images show that at lower fluencies the damage appears as a smooth swelling of the samples surface, with subsequent formation of a bump of molten material; only at higher fluencies evaporation is present with a potential formation of a crater. Build-up of

TABLE I. Aperiodic capping-layer structures and related optical performances.

CL label	Structure	R at 13.5 nm	FRR
CL1	Pt (2 nm) a-Si (8.4 nm)	0.52	15.41
CL2	Pd (2 nm) a-Si (8.4 nm)	0.59	43.70
CL3	Pd (2 nm) Mo (2 nm) a-Si (8.4 nm)	0.60	27.13
CL4	B$_4$C (2 nm) a-Si (34 nm) Mo (3.88 nm)	0.52	10.9

TABLE II. Experimental parameters of the LPP EUV source.

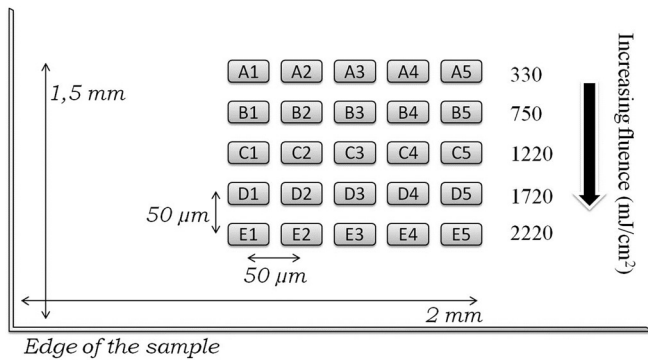|	
Wavelength	13.5 nm
Pulse duration	8.8 ns FWHM
Repetition rate	1 Hz
Spectral filtering	2 nm, selected by two multilayers
EUV spot size	2.65 μm × 5.45 μm FWHM
EUV fluence	$\leq$2.2 J/cm^2 (without Zr filter)

FIG. 2. Map of samples irradiated areas during the experimental session.

splashes of fused material is also present at the border of the damaged spot. This behavior can be possibly attributed to a thermal damage mechanism, with fusion and then evaporation of material, probably favored by the presence of heavy metals with low stiffness and relatively low melting point (Table III).

At highest fluencies some images indicate the presence of big bubbles (Fig. 5) on the irradiated area (CL1: spots E3 and E4; CL2: spots D1, D3, E1, E3, and E4). Such phenomenon involves a bigger amount of material than for the simple fusion process and seems to involve an explosive process; the different morphology could therefore be related to a change in the damage mechanisms.

As said, in the case of CL3, the morphology of the damage areas is similar to those described for CL1 and CL2, so characterized by fusion and bump formation. Nevertheless, in this case the craters are smaller and form only at higher fluencies, indicating a higher damage threshold. However, in contrast with the previous cases, at high fluencies an erosion mechanism creates flat and shallow craters around the spots (Fig. 6).

In the case of B_4C capping-layer (CL4), damages of irregular shape are visible at low fluencies, while at higher fluencies depression areas around the centre of the spot are present (Fig. 7). This morphology is similar to those observed in the case of uncapped Mo/Si multilayer[19] with a Si top layer. It can be concluded that the damage in CL4
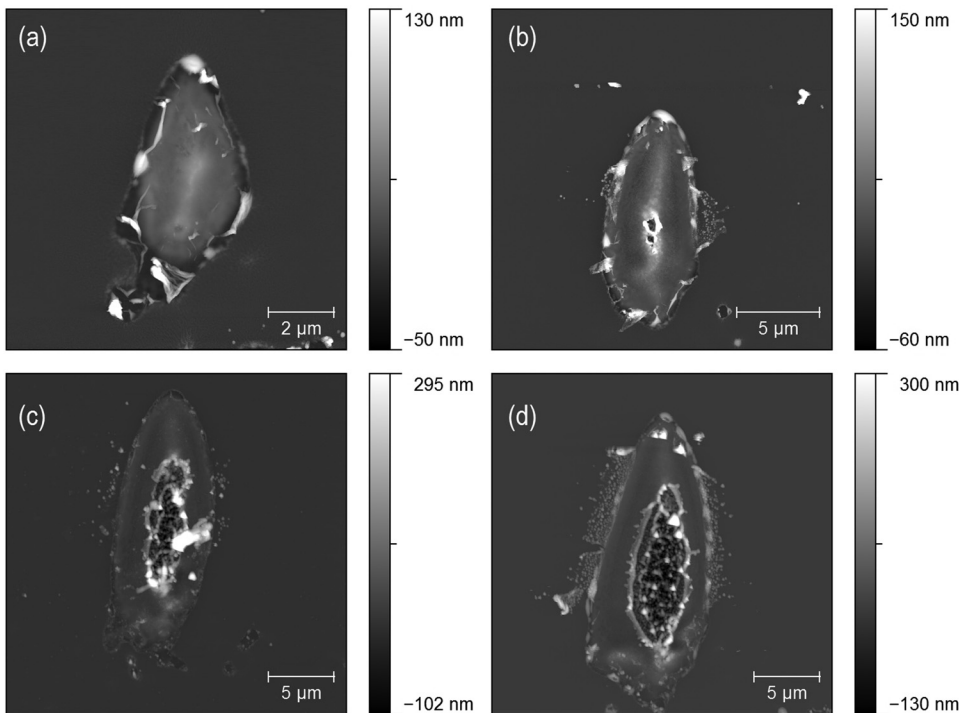

FIG. 3. Topography for CL2 damaged areas, taken at different fluencies: (a) A4 at $F = 330\,mJ/cm^2$; (b) B1 at $F = 750\,mJ/cm^2$; (c) D4 at $F = 1720\,mJ/cm^2$; (d) E2 at $F = 2220\,mJ/cm^2$.
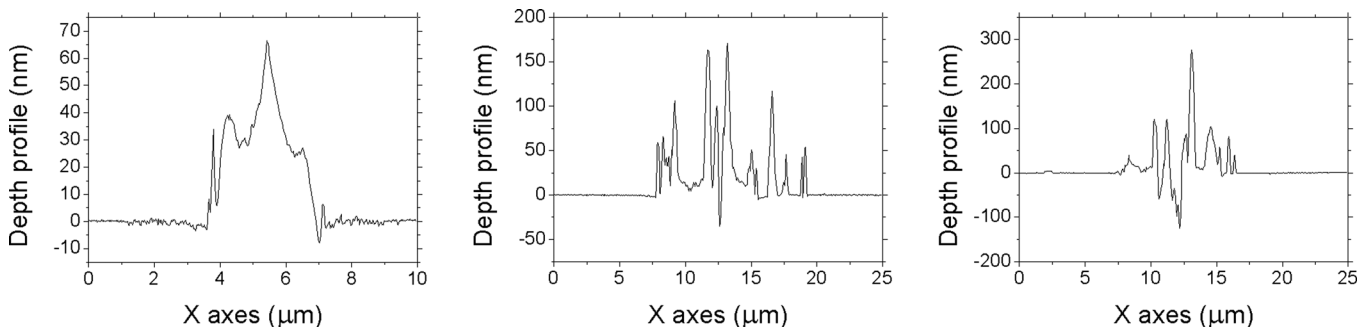

FIG. 4. Selected height profiles for CL2 damaged areas, taken at different fluencies: (a) A4 at $F = 330\,mJ/cm^2$; (b) C2 at $F = 1220\,mJ/cm^2$; (c) D4 at $F = 1720\,mJ/cm^2$.

TABLE III. Confrontation between properties of the materials considered in the experiment (Ref. 26).

Physical property	Pt	Pd	B_4C	Mo	Si
Atomic number	78	46	55.255	42	14
Density (g/cm^3)	21.45	12.02	2.52	10.28	2.32
T_M (°C)	1768.9	1554.9	3036	2623	1414
Thermal conductivity (W/mK)	71.6	71.8	30–42	138	149
Young's module (GPa)	168	121	450–470	329	130–188
Attenuation length at 13.5 (nm)	17.5	23	220	160	580
Lattice constant (Å)	3.920	3.890	5.60	3.150	5.430(cri)
Thermal expansion (K^{-1})	8.8×10^{-6}	11.8×10^{-6}	5×10^{-6}	4.8×10^{-6}	2.6×10^{-6}
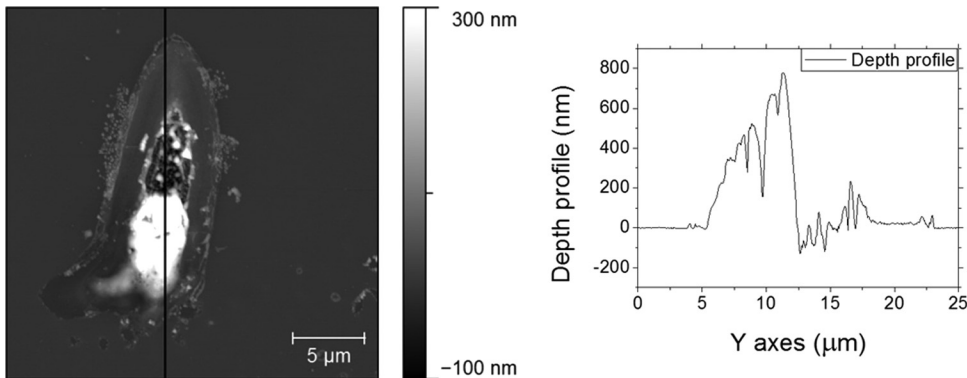
FIG. 5. CL2-D3, $F = 1720 \, \text{mJ/cm}^2$ topography and depth profile.
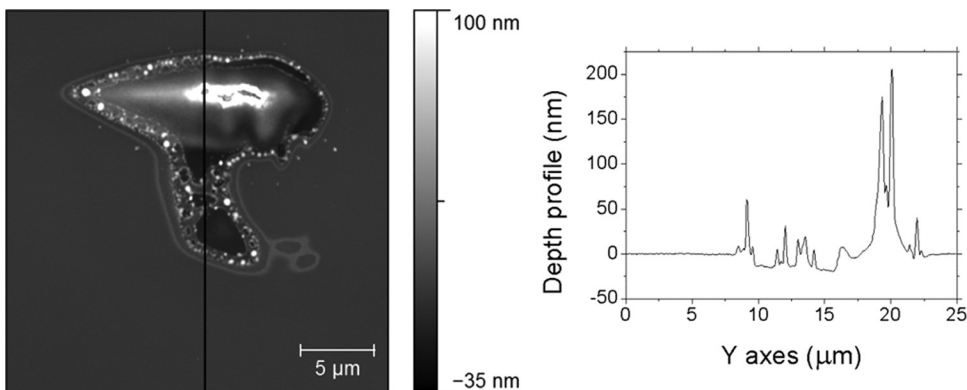
FIG. 6. CL3-E4 at $F = 2220 \, \text{mJ/cm}^2$ topography and depth profile for $F = 2220 \, \text{mJ/cm}^2$.
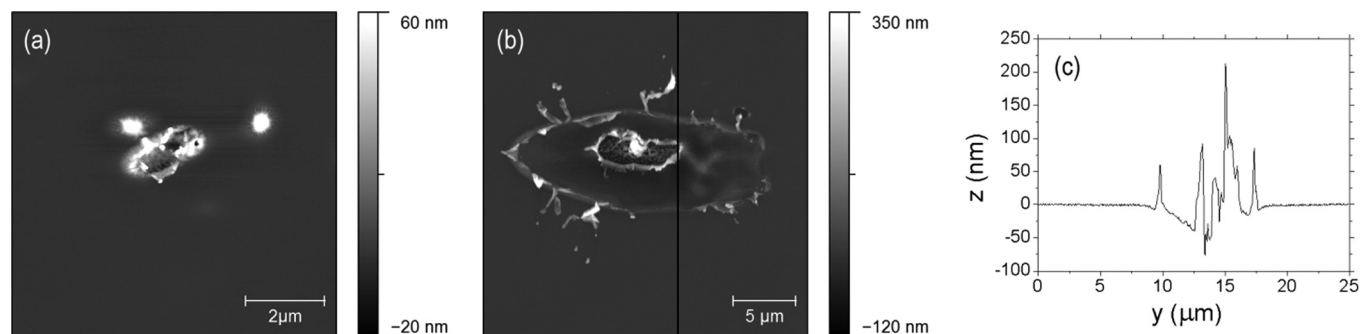
FIG. 7. CL4-A4, $F = 330 \, \text{mJ/cm}^2$ (a) and CL4-E1, $F = 2220 \, \text{mJ/cm}^2$ topography and depth profile.

occurs with a different process than in the case of CL1, CL2, and CL3, being B_4C (and also Si) a non-metallic material.

B. Quantitative analysis of damaging

Volumes of material protruding from the surface as well as crater volume have been considered for a quantitative analysis. On the contrary, the crater depth value has not been taken into account since the damage morphology analysis carried out and described in Sec. III A indicates that generally fluencies used are below the ablation threshold. In Fig. 8 the profile section of a damaged spot useful to understand how volumes have been calculated is reported. In light grey
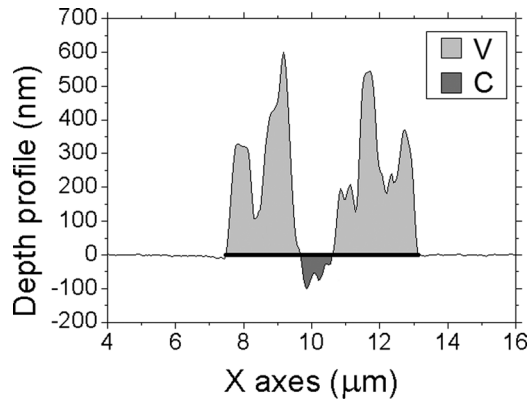
FIG. 8. Profile section of a damaged spot showing the concept of volume calculation.

FIG. 9. Volume versus fluence.

is shown the section of the V volume that is related to the material expanded or condensed over the surface; in dark grey is pictured the section of the crater volume C related to the material removed by the surface.

The factor f = %(C/V) for different fluencies and samples has been calculated. The values reported in Table IV are an average of the five damage volume obtained for each fluence. This factor is used to distinguish the fluencies at which the ablation process is starting and it is prevalent on a thermal mechanism damage. In fact, we assume that when C is above 5%, a significative amount of material is ablated, while below fusion and displacement of material are the more relevant process.

In the case of samples CL1 and CL2, ablation is negligible at all fluencies, and the damage mechanism has a thermal nature while for CL3 and CL4, and above $1720\,mJ/cm^2$ the ablation starts to be dominant; for these samples, the ablation threshold is therefore between 1220 and $1720\,mJ/cm^2$.

In order to define a damage threshold for the different samples, in Fig. 9 a plot of the average volume V versus the irradiation fluencies is reported. The spot considered for the determination of the averaged V are those for which the damaging process is of the same nature, being this fusion of the material with low ablation and absence of explosive behavior. Therefore, the volumes V for fluencies $>1720\,mJ/cm^2$ have been discharged in the case of CL3 and CL4, for what just discussed. Moreover, in the case of CL1 and CL2 and for fluencies above $1720\,mJ/cm^2$, two V values have been calculated: V1, which is the average obtained excluding the damage spots CL1:E3-E4 and CL2:D1-D3-E1-E3-E4, and V2, which is calculated taking into account only these same spots. V1 has

TABLE IV. The factor f at different fluences computed for the samples under investigation. The values reported are an average of the five damage obtained during the experiment.

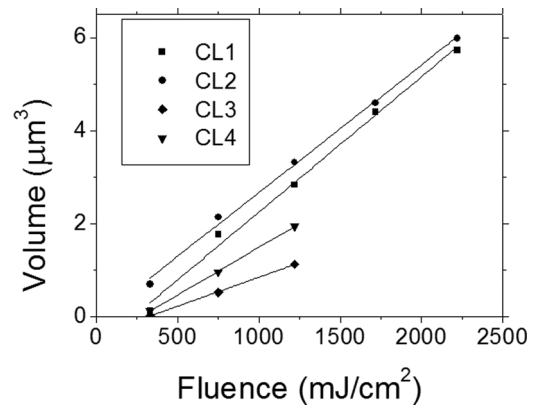| Fluence (mJ/cm^2)	f_{CL1}	f_{CL2}	f_{CL3}	f_{CL4}
330	0	0	1.2	0
750	0	0.014	2	0.13
1220	0.03	0.32	1.8	2.48
1720	0.07	2.89	9.1	36.5
2220	1.1	4.96	16.3	31.8

TABLE V. The volumes V1 and V2 computed for the sample CL1 and CL2 at the fluencies in which the damage mechanism changes.

	CL1		CL2	
Fluence (mJ/cm^2)	V1 (μm^3)	V2 (μm^3)	V1 (μm^3)	V2 (μm^3)
1720	…	…	4.60	10.96
2220	5.72	12.39	5.98	9.63

TABLE VI. Volume data linear fit and damage threshold values.

Sample	Fitting function	Threshold fluence
CL1	$V = (-0.66 \pm 0.18)$ $+ (2.19 \times 10^{-3} \pm 1.2 \times 10^{-4})F$	$F_{th} = 226 \pm 44\,mJ/cm^2$
CL2	$V = (-0.07 \pm 0.12)$ $+ (2.74 \times 10^{-3} \pm 8 \times 10^{-5})F$	$F_{th} = 25 \pm 30\,mJ/cm^2$
CL3	$V = (-0.40 \pm 0.02)$ $+ (1.25 \times 10^{-3} \pm 3 \times 10^{-5})F$	$F_{th} = 319 \pm 25\,mJ/cm^2$
CL4	$V = (-0.56 \pm 0.02)$ $+ (2.04 \times 10^{-3} \pm 3 \times 10^{-5})F$	$F_{th} = 270 \pm 04\,mJ/cm^2$

been reported in Fig. 9, while V1 and V2 data are reported in Table V.

V2 values are two times than V1, due to the big amount of materials displaced in the presence of large bubbles; this confirms the conclusions of the morphologic analysis for which a change in the damage mechanism was observed. In order to determine the damage threshold, a linear fit of the data reported in Fig. 9 has been carried out, and the results are reported in Table VI. CL3 shows the highest damage threshold, while CL2 has a significantly lower one.

IV. CONCLUSIONS

Multilayer samples with different capping layers were irradiated with a focused beam at 13.5 nm, and the damaging of their surface was studied by atomic force microscopy. In fact, since Pd and Mo have similar physical properties (see Table VI, lattice constant and thermal expansion coefficient) thermal and mechanical stresses are reduced, leading to improved stack resistance. The B_4C cap-layer also provides a protection to damage due to its high hardness and the low absorption; at the same time, its lattice constant is similar to

that of the Si material of the layer underneath, making the interface of CL4 highly resistant. The CL1 and CL2 multilayers present more relevant damages; during irradiation, the strong absorption of the two top layer materials increase the energy transferred to the surface, enhancing the damaging effects. In particular, the Pd/Si capped multilayer present a damage threshold of 0.025 J/cm^2; adhesion problem between Pd and Si could eventually explain such lower value.

Comparable damage threshold have been determined in a previous work[20] in which values of (0.09 ± 0.06) J/cm^2 has been determined for a Ru/Si capped multilayer (0.20 ± 0.06) J/cm^2, X for a standard Mo/Si, and (0.26 ± 0.04) J/cm^2 for a Mo/C/Si/C multilayer.

For damaging with pulses in the fs range[21,22] the mechanism is completely different since the material does not have the time to melt; therefore, formation of bubbles and swelling are blocked, and a crater of regular shape is formed.[27] Damage threshold for a Mo/Si ML irradiated at 13.5 nm with a 10 fs pulses at DESY–FLASH is about 45 mJ/cm^2. It must be considered that the velocity of the energy transfer prevents heat dissipation and lower damage threshold would be appeared also for capped multilayer of irradiated in the femtosecond regime.

ACKNOWLEDGMENTS

[1]M. Suman, M. G. Pelizzo, P. Nicolosi, and D. L. Windt, "Aperiodic multilayers with enhanced reflectivity for extreme ultraviolet lithography," Appl. Opt. **47**(16), 2906–2914 (2008).

[2]D. L. Windt, S. Donguy, J. Seely, and B. Kjornrattanawanich, "Experimental comparison of extreme-ultraviolet multilayers for solar physics," Appl. Opt. **43**(9), 1835–1848 (2004).

[3]M. Suman, F. Frassetto, P. Nicolosi, and M. G. Pelizzo, "Design of aperiodic multilayer structures for attosecond pulses in the extreme ultraviolet," Appl. Opt. **46**(33), 8159–8169 (2007).

[4]M. G. Pelizzo, A. J. Corso, G. Monaco, P. Nicolosi, M. Suman, P. Zuppella, and D. Cocco, "Multilayer optics to be used as FEL fundamental suppressors for harmonics selection," Nucl. Instrum. Methods Phys. Res. A **635**, S24–S29 (2011).

[5]Q. Zhong, W. B. Li, Z. Zhang, J. T. Zhu, Q. S. Huang, H. C. Li, Z. S. Wang, P. Jonnard, K. Le Guen, J. M. Andre, H. J. Zhou, and T. L. Huo, "Optical and structural performance of the Al(1% wt Si)/Zr reflection multilayers in the 17-19 nm region," Opt. Express **20**(10), 10692–10700 (2012).

[6]P. Zuppella, G. Monaco, A. J. Corso, P. Nicolosi, D. L. Windt, V. Bello, G. Mattei, and M. G. Pelizzo, "Iridium/silicon multilayers for EUV applications in the 20-35 nm wavelength range," Opt. Lett. **36**(7), 1203–1205 (2011).

[7]R. Soufli, M. Fernandez-Perea, S. L. Baker, J. C. Robinson, J. Alameda, and C. C. Walton, "Spontaneously intermixed Al-Mg barriers enable corrosion-resistant Mg/SiC multilayer coatings," Appl. Phys. Lett. **101**(4), 043111 (2012).

[8]N. A. Papadogiannis, B. Witzel, C. Kalpouzos, and D. Charalambidis, "Observation of attosecond light localization in higher order harmonic generation," Phys. Rev. Lett. **83**, 4289–4292 (1999).

[9]P. Antoine, A. L'Huillier, and M. Lewenstein, "Attosecond pulse trains using high-order harmonics," Phys. Rev. Lett. **77**, 1234–1237 (1996).

[10]M. Suman, G. Monaco, M. G. Pelizzo, D. L. Windt, and P. Nicolosi, "Realization and characterization of an XUV multilayer coating for attosecond pulses," Opt. Express **17**(10), 7922–7932 (2009).

[11]M. Hofstetter, A. Aquila, M. Schultze, A. Guggenmos, S. Yang, E. Gullikson, M. Huth, B. Nickel, J. Gagnon, V. S. Yakovlev, E. Goulielmakis, F. Krausz, and U. Kleineberg, "Lanthanum-molybdenum multilayer mirrors for attosecond pulses between 80 and 130 eV," New J. Phys. **13**, 063038 (2011).

[12]C. Bourassin-Bouchet, S. De Rossi, J. Wang, E. Meltchakov, A. Giglia, N. Mahne, S. Nannarone, and F. Delmotte, "Shaping of single-cycle sub-50-attosecond pulses with multilayer mirrors," New J. Phys. **14**, 023040 (2012).

[13]B. Vodungbo, A. B. Sardinha, J. Gautier, G. Lambert, C. Valentin, M. Lozano, G. Iaquaniello, F. Delmotte, S. Sebban, J. Lüning, and P. Zeitoun, "Polarization control of high order harmonics in the EUV photon energy range," Opt. Express **19**(5), 4346–4356 (2011).

[14]H. N. Chapman, S. P. Hau-Riege, M. J. Bogan, S. Bajt, A. Barty, S. Boutet, S. Marchesini, M. Frank, B. W. Woods, W. H. Benner, R. A. London, U. Rohner, A. Szoke, E. Spiller, T. Moller, C. Bostedt, D. A. Shapiro, M. Kuhlmann, R. Treusch, E. Plonjes, F. Burmeister, M. Bergh, C. Caleman, G. Huldt, M. M. Seibert, and J. Hajdu, "Femtosecond time-delay X-ray holography," Nature **448**(7154), 676–679 (2007).

[15]E. Allaria, C. Callegari, D. Cocco, W. M. Fawley, M. Kiskinova, C. Masciovecchio, and F. Parmigiani, "The FERMI@ELETTRA free-electron-laser source for coherent x-ray physics: photon properties, beam transport system and applications," New J. Phys. **12**, 075002 (2010).

[16]A. J. Corso, P. Zuppella, D. L. Windt, M. Zangrando, and M. G. Pelizzo, "Extreme ultraviolet multilayer for the FERMI@ELETTRA free electron laser beam transport system," Opt. Express **20**(7), 8006–8014 (2012).

[17]M. Suman, G. Monaco, P. Zuppella, P. Nicolosi, M. G. Pelizzo, F. Ferrari, M. Lucchini, and M. Nisoli, "Analysis of the damage effect of femtosecond-laser irradiation on extreme ultraviolet Mo/Si multilayer coating," Thin Solid Films **520**(6), 2301–2306 (2012).

[18]A. Giglia, N. Mahne, A. Bianco, C. Svetina, and S. Nannarone, "EUV soft X-ray characterization of a FEL multilayer optics damaged by multiple shot laser beam," Nucl. Instrum. Methods Phys. Res. A **635**, S30–S38 (2011).

[19]F. Barkusky, A. Bayer, S. Döring, P. Grossmann, and K. Mann, "Damage threshold measurements on EUV optics using focused radiation from a table-top laser produced plasma source," Opt. Express **18**(5), 4346–4355 (2010).

[20]M. Müller, F. Barkusky, T. Feigl, and K. Mann, "EUV damage threshold measurements of Mo/Si multilayer mirrors," Appl. Phys. A **108**(2), 263–267 (2012).

[21]A. R. Khorsand, R. Sobierajski, E. Louis, S. Bruijn, E. D. van Hattum, R. W. E. van de Kruijs, M. Jurek, D. Klinger, J. B. Pelka, L. Juha, T. Burian, J. Chalupsky, J. Cihelka, V. Hajkova, L. Vysin, U. Jastrow, N. Stojanovic, S. Toleikis, H. Wabnitz, K. Tiedtke, K. Sokolowski-Tinten, U. Shymanovich, J. Krzywinski, S. Hau-Riege, R. London, A. Gleeson, E. M. Gullikson, and F. Bijkerk, "Single shot damage mechanism of Mo/Si multilayer optics under intense pulsed XUV-exposure," Opt. Express **18**(2), 700–712 (2010).

[22]R. Sobierajski, S. Bruijn, A. R. Khorsand, E. Louis, R. W. E. van de Kruijs, T. Burian, J. Chalupsky, J. Cihelka, A. Gleeson, J. Grzonka, E. M. Gullikson, V. Hajkova, S. Hau-Riege, L. Juha, M. Jurek, D. Klinger, J. Krzywinski, R. London, J. B. Pelka, T. Plocinski, M. Rasinski, K. Tiedtke, S. Toleikis, L. Vysin, H. Wabnitz, and F. Bijkerk, "Damage mechanisms of MoN/SiN multilayer optics for next-generation pulsed XUV light sources," Opt. Express **19**(1), 193–205 (2011).

[23]A. J. Corso, P. Zuppella, P. Nicolosi, D. L. Windt, E. M. Gullikson, and M. G. Pelizzo, "Capped Si/Mo multilayers with improved performances at 30.4 nm for future solar missions," Opt. Express **19**(15), 13963–13973 (2011).

[24]M. G. Pelizzo, A. J. Corso, P. Zuppela, and P. Nicolosi, "Multilayer coatings and their use in spectroscopic applications," Nucl. Instrum. Methods Phys. Res. A (in press).

[25]D. L. Windt and W. K. Waskiewicz, "Multilayer facilities required for extreme-ultraviolet lithography," J. Vac. Sci. Technol. B **12**(6), 3826–3832 (1994).

[26]See http://www.infoplease.com/periodictable.php?id=46 for an interactive periodic table with the main physical parameters for each element (last accessed 2012).

[27]J. C. Miller and R. F. Haglund, *Laser Ablation and Desorption* (Academic Press, 1998).